Large-scale production and study of a synthetic G protein-coupled receptor: Human olfactory receptor 17-4

Brian L. Cook[a,1], Dirk Steuerwald[a], Liselotte Kaiser[a], Johanna Graveland-Bikker[a], Melanie Vanberghem[a], Allison P. Berke[a], Kara Herlihy[b], Horst Pick[c], Horst Vogel[c], and Shuguang Zhang[a,1]

[a]Department of Biological Engineering, and Center for Biomedical Engineering, Massachusetts Institute of Technology, Cambridge, MA 02139-4307; [b]Biacore Life Sciences, GE Healthcare, 800 Centennial Avenue, Piscataway, NJ 08854; and [c]Institut des Sciences et Ingénierie Chimiques, Ecole Polytechnique Fédérale de Lausanne (EPFL), CH-1015, Lausanne, Switzerland

Edited by Alexander Varshavsky, California Institute of Technology, Pasadena, CA, and approved May 4, 2009 (received for review November 22, 2008)

Although understanding of the olfactory system has progressed at the level of downstream receptor signaling and the wiring of olfactory neurons, the system remains poorly understood at the molecular level of the receptors and their interaction with and recognition of odorant ligands. The structure and functional mechanisms of these receptors still remain a tantalizing enigma, because numerous previous attempts at the large-scale production of functional olfactory receptors (ORs) have not been successful to date. To investigate the elusive biochemistry and molecular mechanisms of olfaction, we have developed a mammalian expression system for the large-scale production and purification of a functional OR protein in milligram quantities. Here, we report the study of human OR17-4 (hOR17-4) purified from a HEK293S tetracycline-inducible system. Scale-up of production yield was achieved through suspension culture in a bioreactor, which enabled the preparation of >10 mg of monomeric hOR17-4 receptor after immunoaffinity and size exclusion chromatography, with expression yields reaching 3 mg/L of culture medium. Several key post-translational modifications were identified using MS, and CD spectroscopy showed the receptor to be ≈50% α-helix, similar to other recently determined G protein-coupled receptor structures. Detergent-solubilized hOR17-4 specifically bound its known activating odorants lilial and floralozone in vitro, as measured by surface plasmon resonance. The hOR17-4 also recognized specific odorants in heterologous cells as determined by calcium ion mobilization. Our system is feasible for the production of large quantities of OR necessary for structural and functional analyses and research into OR biosensor devices.

BiacoreA100 | detergent screen | fos-choline 14 | G protein-coupled receptor purification | membrane protein

Animal noses have evolved the ability to rapidly detect a seemingly infinite array of odors at minute concentrations. The basis of this sensitivity are the olfactory (smell) receptors, a large class of G protein-coupled receptors (GPCRs) that function together combinatorially to allow discrimination between a wide range of volatile and soluble molecules (1, 2). As GPCRs, all olfactory receptors (ORs) are integral membrane proteins with 7 predicted transmembrane domains. To date, crystal structures exist for only 5 GPCR proteins (3). Despite the fact that ORs represent the largest class of known membrane proteins, no detailed structure exists for any OR, because the major obstacle to structural and functional studies on membrane proteins is the notorious difficulty involved in expressing and purifying the large quantities of receptor protein sample required for techniques such as X-ray crystallography. The first crucial step to enable such pivotal biochemical and structural analyses is to engineer systems with the capacity to produce and purify milligram quantities of an OR.

hOR17-4 (alternately known as OR1D2) is of particular interest because, in addition to olfactory neurons, it is expressed on the midpiece of human spermatozoa (4). Sperm expressing hOR17-4 were found to migrate toward known hOR17-4 odorant ligands such as bourgeonal, lilial, and floralozone (4). Thus, the receptor serves a dual role in that it recognizes odorants in the nose and plays a potential role in sperm chemotaxis and fertilization. Structural studies of hOR17-4 would not only provide information crucial to understanding the molecular basis of olfaction, but also have application to human reproduction.

We recently developed an OR expression system (5) using stably-inducible mammalian HEK293S (human embryonic kidney) cell lines by optimizing methods originally developed in the Khorana lab (6, 7) at the Massachusetts Institute of Technology to generate milligram quantities of functional rhodopsin. In adherent culture, this adapted rho-tag system was used to express and purify monomeric hOR17-4 to >90% purity (5). Here, we report that this system can be scaled up by using bioreactor culture to facilitate the production and purification of milligram amounts of hOR17-4. Key to the efficient extraction of hOR17-4 was a comprehensive screen of diverse detergents and the selection of zwitter-ionic fos-choline detergents as solubilizing agents, because all nonionic detergents tested proved ineffective. The purified hOR17-4 protein was structurally and functionally characterized by using several spectroscopy methods.

Results

Construction of Stable hOR17-4-Inducible HEK293S GnTI$^-$ Cell Lines. We recently described the fabrication of a synthetic hOR17-4 gene using PCR-based gene synthesis and the subsequent construction of stable HEK293S cell lines with tetracycline-inducible expression of the hOR17-4 receptor protein (5). When induced with a combination of tetracycline and sodium butyrate, these HEK293S cells generate >30 μg of hOR17-4 per 15-cm plate. However, when assayed by SDS/PAGE, the receptor monomer migrated as a doublet at ≈30 and 32 kDa (the full-length rho-tagged hOR17-4 protein, with theoretical molecular mass of 36.2 kDa, migrates slightly faster on SDS/PAGE gels). Our initial hypothesis was that the 32-kDa band constituted a glycosylated form of the receptor. Because heterogeneity could potentially interfere with future structural analysis and crystallization, we sought to achieve a homogeneous glycosylation pattern by porting the hOR17-4-inducible expression system into a HEK293S *N*-acetylglucosaminyltransferase I-negative (GnTI$^-$) cell line shown to produce homogeneously glycosylated rhodopsin (8). During colony screening we isolated subclonal strains that exclusively expressed the slower migrating (32 kDa) form of the receptor even under high-level expression (Fig. 1*A*).

Author contributions: B.L.C., D.S., L.K., J.G.-B., K.H., H.P., H.V., and S.Z. designed research; B.L.C., D.S., L.K., J.G.-B., M.V., A.P.B., K.H., and H.P. performed research; K.H., H.P., and H.V. contributed new reagents/analytic tools; B.L.C., D.S., L.K., J.G.-B., M.V., K.H., H.P., H.V., and S.Z. analyzed data; and B.L.C., L.K., J.G.-B., H.P., and S.Z. wrote the paper.

The authors declare no conflict of interest.

This article is a PNAS Direct Submission.

[1]To whom correspondence may be addressed. E-mail: cookb@mit.edu or shuguang@mit.edu.

This article contains supporting information online at www.pnas.org/cgi/content/full/0811089106/DCSupplemental.

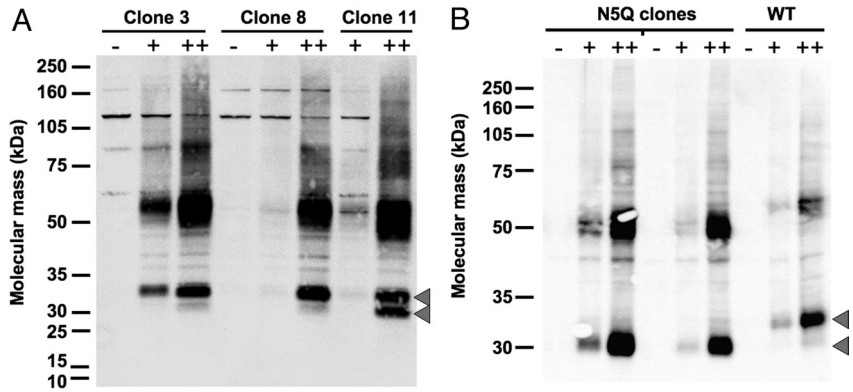

Fig. 1. Construction of hOR17-4-inducible HEK293S GnT1$^{-/-}$ cell lines for use in liquid bioreactor culture. Clones were tested for induction after 48 h in plain media (−) or media supplemented with 1 μg/mL tetracycline (+) or tetracycline plus 5 mM sodium butyrate enhancer (++). Arrows indicate the positions of the 32- and 30-kDa monomer forms. (*A*) Levels of hOR17-4 were probed via SDS/PAGE Western blot analysis against the rho tag (rho1D4 mAb). Clones 3 and 8 show high levels of induction after the addition of sodium butyrate but have low levels of the potentially unglycosylated 30-kDa monomer form of hOR17-4, unlike clone 11 and previous clones in the HEK293S system. Clone 3 was selected for subsequent bioreactor experiments. (*B*) To investigate the potential N-linked glycosylation of hOR17-4, the consensus glycosylation sequence (-Asn-Gln-Ser-) was altered by site-directed mutagenesis to change the asparagine at position 5 to glutamine (N5Q mutation). After the generation of new stable hOR17-4(N5Q)-inducible clones, the SDS/PAGE migration pattern of receptor monomer was compared with wild type after induction. Mutation of the glycosylation site (N5Q) eliminated the upper form (32 kDa) of hOR17-4 monomer and only the lower form (30 kDa) is present, indicating the size discrepancy is indeed caused by glycosylation on Asn-5.

ORs possess a conserved N-linked glycosylation consensus sequence (Asn-X-Ser/Thr) at their N termini (9), and the resulting glycosylation may be important for receptor functionality and proper folding (10), as is the case for other GPCRs (11). To investigate whether the observed size discrepancy was caused by N-linked glycosylation, we generated a stable cell line that expressed a mutated form of hOR17-4 (N5Q) where the consensus asparagine was replaced by a glutamine. This hOR17-4 N5Q mutant ran solely at 30 kDa with no 32-kDa form present (Fig. 1*B*), indicating that the 32-kDa form of wild-type hOR17-4 is N-glycosylated on Asn-5. However, as a lack of glycosylation could potentially compromise receptor function, all subsequent experiments were performed with the wild-type hOR17-4-inducible cell line (clone 3; Fig. 1*A*).

Detergent Screening and Optimization of hOR17-4 Solubilization from HEK293S Cells. Initial transient transfection into HEK293S cells and subsequent solubilization using the detergent dodecyl maltoside (DDM), which has been successfully used to solubilize several other GPCRs (6–8, 12), revealed low levels of hOR17-4 protein yield compared with constructs encoding opsin. To investigate whether DDM was insufficient to solubilize hOR17-4, we performed a large detergent screen that included representatives from the nonionic, zwitter-ionic, polar, and ionic detergent classes. Immunoblot analysis showed that the majority of commercially available detergents were poor choices for extracting the hOR17-4 GPCR protein from HEK293S cells (Fig. 2). However, the fos-choline class of detergents proved highly effective and showed a clear relationship between chain length and solubilization yield, with fos-choline-16 (FC16) showing a >10-fold increase over DDM. However, the critical micelle concentration (CMC) of FC16 is so low (0.00053% wt/vol) as to make any subsequent detergent exchange nearly impossible. Therefore, fos-choline-14 (FC14), with a CMC ≈10 times higher (0.0046% wt/vol) was selected as optimal solubilization agent. Importantly, FC14 showed greater hOR17-4 yield than solubilization with harsher ionic detergents such as sarcosine and deoxycholate. The fos-choline detergents are structurally related to

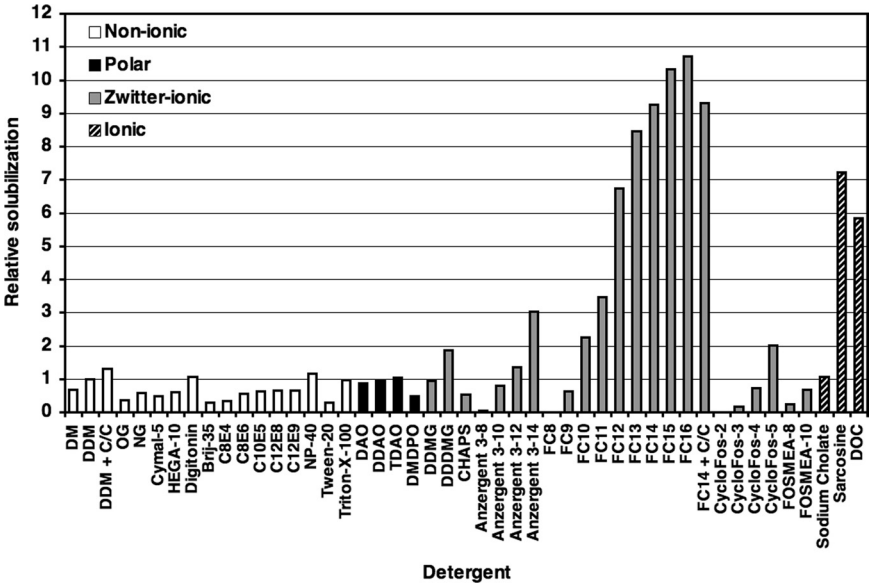

Fig. 2. Detergent screen for optimal solubilization of hOR17-4 expressed in HEK293S cells. Expression of hOR17-4 was induced with tetracycline (1 μg/mL) and sodium butyrate (5 mM) for 48 h and receptors were solubilized in PBS containing detergent(s) for 4 h at 4 °C. All detergents were used at a concentration of 2% (wt/vol) unless otherwise indicated. Relative solubilization corresponds to the fold increase over DDM in solubilizing hOR17-4 monomer/dimer. Detergent abbreviations used are: DM, decyl maltoside; C/C, CHAPS (1%) and cholesterol hemisuccinate (0.2%); OG, octyl glucoside; NG, nonyl glucoside; DAO, n-decyl-*N*,*N*-dimethylamine-*N*-oxide; DDAO, n-dodecyl-*N*,*N*-dimethylamine-*N*-oxide; TDAO, n-tetradecyl-*N*,*N*-dimethylamine-*N*-oxide; DMDPO, dimethyldecylphosphine oxide; DDMG, n-decyl-*N*-*N*-dimethylglycine; DDDMG, n-dodecyl-*N*-*N*-dimethylglycine; sarcosine, sodium dodecanoyl sarcosine; DOC, deoxycholate.

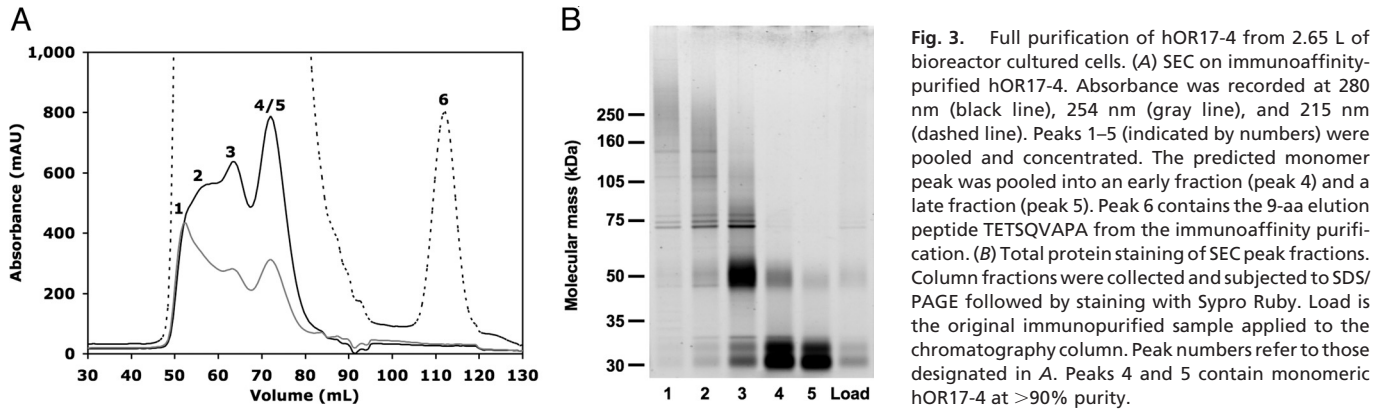

Fig. 3. Full purification of hOR17-4 from 2.65 L of bioreactor cultured cells. (*A*) SEC on immunoaffinity-purified hOR17-4. Absorbance was recorded at 280 nm (black line), 254 nm (gray line), and 215 nm (dashed line). Peaks 1–5 (indicated by numbers) were pooled and concentrated. The predicted monomer peak was pooled into an early fraction (peak 4) and a late fraction (peak 5). Peak 6 contains the 9-aa elution peptide TETSQVAPA from the immunoaffinity purification. (*B*) Total protein staining of SEC peak fractions. Column fractions were collected and subjected to SDS/PAGE followed by staining with Sypro Ruby. Load is the original immunopurified sample applied to the chromatography column. Peak numbers refer to those designated in *A*. Peaks 4 and 5 contain monomeric hOR17-4 at >90% purity.

phosphatidylcholine (PC), a phospholipid and major constituent of the lipid bilayer of mammalian cells. Additional solubilization yield studies were carried out to determine the optimal FC14 concentration and extraction buffer. Addition of glycerol or increasing salt concentration was found to substantially decrease receptor yield.

After solubilization of hOR17-4 from native cell membranes, we attempted to exchange the zwitter-ionic fos-choline for the milder nonionic DDM during the immunoaffinity bead immobilization, because DDM has been successfully used to keep many other GPCRs soluble. However, this process resulted in a near total loss of hOR17-4 yield because of aggregation, indicating that FC14 is crucial not only for OR extraction but for the maintenance of the solubility of OR proteins in solution. All subsequent purifications used FC14 exclusively.

Milligram-Scale Bioreactor Production of hOR17-4 and Subsequent Purification. The use of adherent cell culture for milligram-scale purification of the receptor monomer poses a substantial challenge, because many hundreds of plates would be required. Because the HEK293S GnTI$^-$ cell line is capable of suspension culture at high cell densities, we chose to scale-up production by using a bioreactor and methods previously optimized for the milligram-scale production of bovine rhodopsin (12). Each bioreactor run consisted of 1.25 L of culture media inoculated with hOR17-4-inducible HEK293S GnTI$^-$ cells at an initial density of $6–8 \times 10^5$ cells per mL. The media was supplemented on day 5, and hOR17-4 expression was induced on day 6 by using tetracycline and sodium butyrate and harvested 40 h later (day 8). Cell density at time of induction was 6.0×10^6 cells per mL and had increased to 9.6×10^6 cells per mL at the time of harvest. Thus, a single 1.25-L bioreactor run produced 12 billion cells (a cell pellet of 16 g), the equivalent of ≈200 15-cm tissue culture plates.

Cell pellets from 2 separate bioreactor runs were combined and subjected to solubilization by using FC14 (molecular mass = 379.5) followed by immunoaffinity purification with the rho1D4 monoclonal antibody (mAb) conjugated to Sepharose beads to capture the rho-tagged hOR17-4 protein. The eluate (containing 10.3 mg of hOR17-4) was then subjected to size exclusion chromatography (SEC) to isolate the monomeric receptor fraction by using gel filtration. Several peaks were observed (Fig. 3*A*) and were found to correspond to aggregate, dimeric, and monomeric receptor (Fig. 3*B*). The dimeric and monomer peaks eluted at 63.4 mL (0.51 column volumes (CV)) and 72.1 mL (0.58 CV), respectively, which was identical to that observed in our hOR17-4 purification using adherent culture (5). Using gel filtration standards we estimated the apparent masses of the hOR17-4-detergent complexes at 140 kDa (monomer) and 275 kDa (dimer), indicating that each hOR17-4 protein unit is solubilized in a complex with ≈270 molecules of FC14 (2.8 g of FC14 per g of protein). Although this number might seem high, the mass of detergent bound to most membrane proteins is far greater than the detergent micellar mass (i.e., ≈47 kDa for FC14) (13). For example, monomeric rhodopsin/DDM complexes are ≈126 kDa (14). Were our 140-kDa complex to contain dimeric hOR17-4, each would be complexed with ≈90 molecules of FC14 that is well below the aggregation number of 120 (14). Thus, we believe that the 2 peaks at 0.51 and 0.58 CV represent dimeric and monomeric receptor–detergent complexes, respectively.

Peak fractions were collected, pooled, concentrated, and subjected to SDS/PAGE (Fig. 3*B*). The final yield of hOR17-4 monomer was 2.68 mg at >90% purity, the only other band visible being dimeric hOR17-4. Additionally, the putative dimer peak contained a total of 2.45 mg of largely dimeric receptor. Importantly, the appearance of monomer form in earlier peaks is likely caused by the effect of SDS dissociating the dimeric and oligomeric receptor forms during gel electrophoresis.

After the initial milligram-scale purification, we repeated the experiment with 2 additional bioreactor runs (2.5 L of suspension culture). However, a large excess of rho1D4-Sepharose beads (60 mL of bead slurry, total binding capacity 42 mg) was added to ensure complete capture of solubilized hOR17-4. Total yield of receptor after immunoaffinity chromatography was 30.5 mg, which led to the purification of 7.5 mg of hOR17-4 monomer after gel filtration chromatography. This constitutes nearly a 3-fold increase over the first run and a yield of ≈3 mg/L for purified hOR17-4 monomer, which approaches yields of rhodopsin and rhodopsin mutants when similarly expressed (7). The resulting OR protein is at sufficiently high purity (>90%) for immediate concentration and application to crystallization screening.

Spectroscopic Characterization of Purified hOR17-4. We next sought to test whether the purified, FC14-solubilized hOR17-4 retained proper structure and functionality. Our prediction for hOR17-4 secondary structure, based on structural modeling (15) and transmembrane domain calculations (www.uniprot.org/uniprot/P34982), was ≈50% α-helix. When subjected to far-UV CD spectroscopy, the monomeric hOR17-4 displayed a spectrum characteristic of a predominantly α-helical protein with minima at 208 and 222 nm (Fig. 4*A*). Analysis of the spectrum using the K2D algorithm (16) returned values of 49% α-helix, 18% β-sheet, and 33% random coil content, in agreement with predicted hOR17-4 secondary structure.

The ability to purify milligram quantities of hOR17-4 also allowed us to probe tertiary structure using near-UV CD spectroscopy (Fig. 4*B*). Several significant peaks were observed that suggest a defined tertiary structure for the OR. Wild-type opsin has similar near-UV peaks in this region, whereas functionally inactive opsin mutants showed flat spectra, indicating misfolded protein (17). Characterization by tryptophan fluorescence spectroscopy using excitation at 280 nm showed an emission maximum at 335 nm, which is similar to the value experimentally determined for rat OR5 of 328 nm (18).

hOR17-4 Activation Monitored by Intracellular Calcium-Ion Mobility Assay. Because the C-terminal rho tag could potentially interfere with G protein-mediated signal transduction, we also confirmed that our

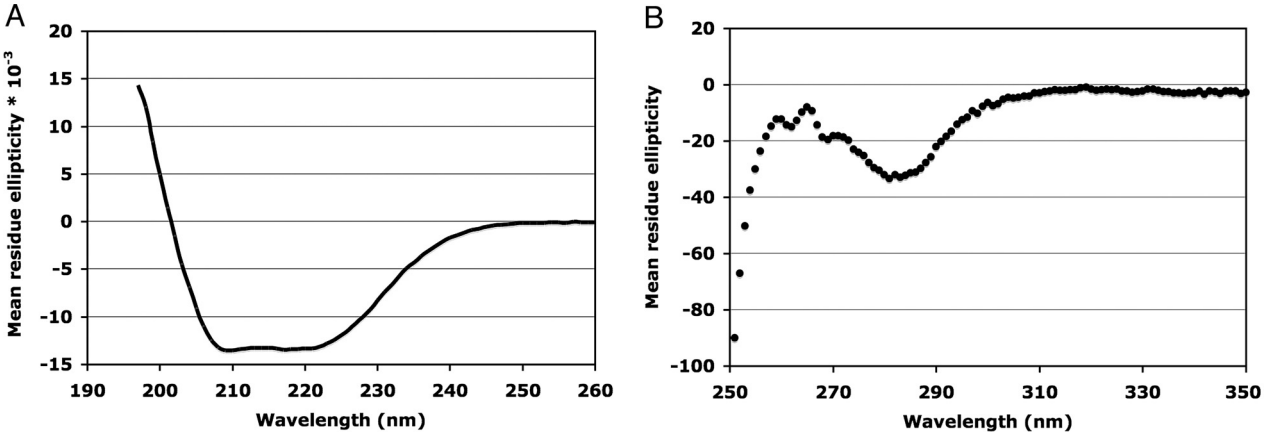

Fig. 4. Characterization of purified hOR17-4 by CD spectroscopy. Purified hOR17-4 monomer was analyzed by both far-UV and near-UV CD spectroscopy. Mean residue ellipticity [θ] has units of degree $\times$ cm^2 $\times$ dmol^{-1}. (*A*) Far-UV CD spectrum of hOR17-4 displaying secondary structure of 49% α-helix. Spectrum shown is the average of 5 replicate scans. (*B*) Near-UV CD spectrum of hOR17-4 showing distinct tertiary structure peaks. Functional bovine rhodopsin has a similar peak in this region, whereas nonfunctional opsin mutants show flat spectra characteristic of a misfolded globular state.

synthetic hOR17-4 displayed wild-type function in the HEK293S cell membranes. The functional activity and specificity of hOR17-4 was probed in heterologous HEK293S cells by monitoring intracellular calcium ion concentrations by time-lapse confocal microscopy (19). In our HEK293S cells, ORs can signal through the inositol triphosphate (IP_3) pathway to release intracellular Ca^{2+} from the ER, mediated by the "promiscuous" G protein $G_{\alpha q}$. Induced cells responded to the specific odorant bourgeonal at concentrations as low as 1 μM (Fig. 5). Odorant response could be blocked by coapplication of the hOR17-4 antagonist undecanal. No response was seen for the nonspecific odorants octanal and anithole. Importantly, nearly 100% of the cells were responsive to bourgeonal because of the stable-inducible nature of this system, a vast improvement over expression methods that relied on transient transfection with <5% of cells being responsive (3).

Analysis of hOR17-4 Odorant Binding Using SPR. To assay the binding activity of detergent-solubilized hOR17-4, we developed an assay by using surface plasmon resonance (SPR) to demonstrate that the solubilized receptor retains selectivity in binding odorant ligands in a concentration-dependent manner. First, the rho1D4 mAb was covalently attached to the dextran surface of a Biacore CM4 chip by standard amine-coupling chemistry. The hOR17-4 receptor protein was then noncovalently captured on the antibody via its C-terminal rho tag (TETSQVAPA). Odorant ligands were then applied and odorant binding was detected in real time via the mass-based refractive index change. Solubilized hOR17-4 receptors bound the specific odorants lilial and floralozone in a dose-dependent manner (Fig. 6). Because of low odorant solubility (>40 μM), the equilibrium dissociation constant could not be rigorously determined, but was approximately in the low micromolar range. Low-affinity Biacore data are typically characterized by fast on and off rates, where curvature in the association and dissociation phase may not be observable. The different extents of curvature suggest different kinetic behavior for the 2 compounds, but further experiments would be required to fully characterize these differences. However, the sensorgram data shown reinforce the prediction of low micromolar affinities for the 2 odorants. Additionally, no binding activity was detected for the nonspecific odorant sulfuryl acetate (Fig. 6*A Inset*). Thus, these results indicate that hOR17-4 receptor retains its specific binding activity in the solubilized state.

Characterization of hOR17-4 Posttranslational Modifications. We next used mass spectrometry (chymotrypsin digest followed by LC-MS) to identify any posttranslational modifications. ORs are believed to possess 2 disulfide bonds between 4 conserved cysteine residues located in extracellular loops 1 and 2 (EC1 and EC2) (9). For hOR17-4, these 2 bonds are Cys-97–Cys-179 (EC1–EC2) and Cys-169–Cys-189 (EC2–EC2). Analysis confirmed the presence of the intra-EC2 disulfide bond (Cys-169–Cys-189) predicted for ORs (Table S1). No corresponding

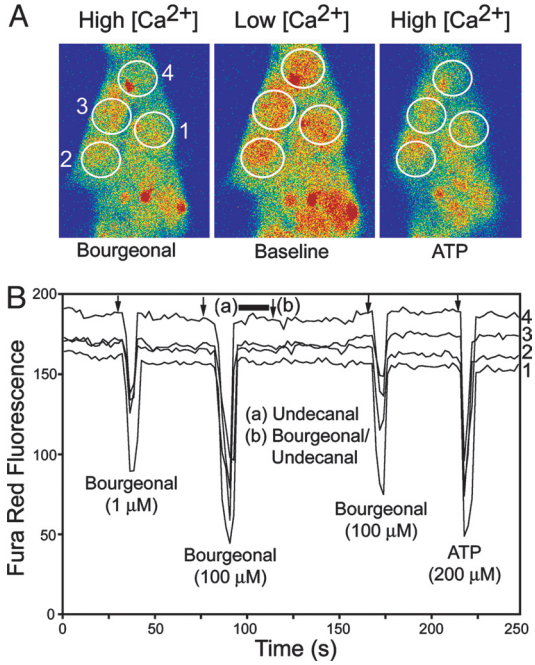

Fig. 5. Calcium-influx assays of cell surface expressed hOR17-4. hOR17-4 expressed in a stable-inducible HEK293S cell line exhibits specific activation by its cognate ligand bourgeonal. (*A*) Transient changes of the cytosolic Ca^{2+} concentration were recorded with a confocal microscopy using Fura-Red (Ex 488 nm/Em 650 nm) as a fluorescent Ca^{2+} indicator. The decrease of the fluorescence signal induced by receptor activation in response to bourgeonal (100 μM) corresponds to an increase of the cytosolic Ca^{2+} concentration. The application of 200 μM adenosine triphosphate (ATP) served as a control of HEK293S cell excitability. (*B*) In a randomly selected field of view, Fura Red fluorescence intensities of odorant-induced Ca^{2+} responses were recorded on 4 individual cells (nos. 1, 2, 3, 4) as a function of time. hOR17-4 induces transient Ca^{2+} signaling to consecutive stimulations by bourgeonal (1 μM; 100 μM). Arrows indicate the time point of odorant application. The preincubation (black bar) with the hOR17-4 antagonist undecanal (100 μM) inhibited hOR17-4 activation by bourgeonal (100 μM) during coapplication (arrow) with undecanal (100 μM). After subsequent odorant washout, cells were again excitable with bourgeonal (100 μM).

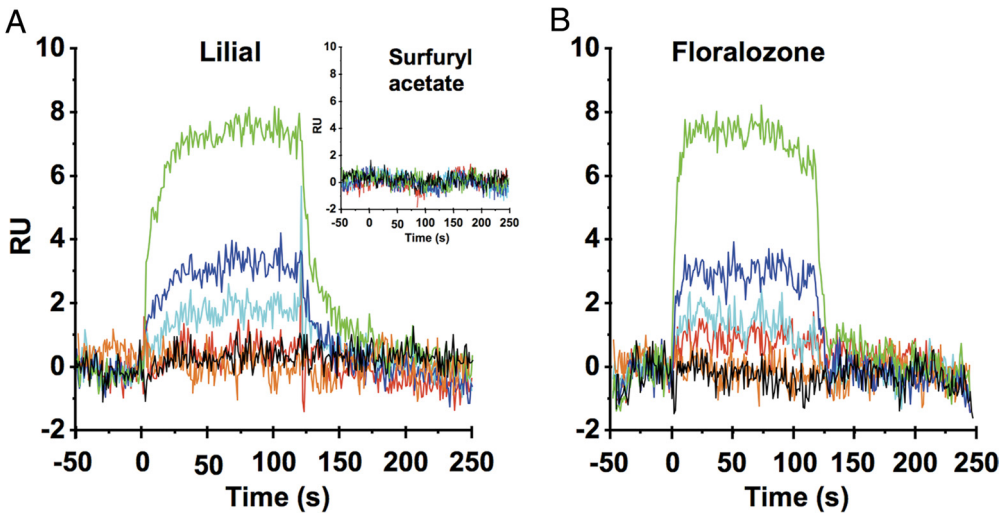

Fig. 6. Probing the binding activity of detergent-solubilized hOR17-4 using SPR. Detection of odorant binding activity of OR was monitored in real time with a Biacore A100 SPR instrument. The hOR17-4 was first captured on the SPR chip surface via a covalently immobilized rho1D4 mAb. Time courses of odorant binding were recorded after odorant application. The receptor bound the specific odorants lilial (*A*) and floralozone (*B*) in a concentration-dependent manner. Odorant binding curves shown are: blank control (black), 5 μM (red), 10 μM (light blue), 20 μM (dark blue), and 40 μM (green). No response was seen for the nonbinding control odorant sulfuryl acetate, as indicated by the 40-μM application (orange curves) and the full series of concentration data (*A Inset*). All results were simultaneously subtracted from a reference channel containing mAb and blank buffer.

unlinked peptides were detected, indicating homogeneity. Presence of the remaining disulfide bond (Cys-97–Cys-179) was unconfirmed, because no corresponding peptides (disulfide-linked or unlinked) were detected, presumably because of the resistance of the detergent-solubilized OR to complete protease digestion.

Additionally, MS determined the N-linked glycosylation present on Asn-5 to be $Man_3GlcNac_3$. This hexasaccharide is also the predominant glycosylation seen in retina-derived bovine opsin on Asn-2 and Asn-15 (20). However, it is worthwhile to note that rhodopsin heterologously prepared with the HEK293S GnTI$^-$ cell line was found to have the N-glycan $Man_5GlcNac_2$ (8), indicating hOR17-4 follows a different glycosylation pathway in this system.

Discussion

Aspects of Glycosylation. The appearance of 2 distinct hOR17-4 monomer bands after purification could pose a problem for structural studies using X-ray diffraction, because typically a high degree of protein homogeneity is required for protein crystallization. We initially believed that it was possible to obtain primarily the 32-kDa form by using the HEK293S GnTI$^-$ cell line clones (Fig. 1*A*). However, the rho1D4 immunoaffinity purification appears to significantly increase the proportion of the 30-kDa monomer form relative to the 32-kDa form, as seen in Fig. 3*B*. One hypothesis is that the 30-kDa (potentially nonglycosylated) form binds more readily to the rho1D4-coupled bead matrix. Therefore, to obtain truly homogeneous hOR17-4 monomer it may be necessary to perform purifications with the hOR17-4 (N5Q) mutant cell line (Fig. 1), where only the 30-kDa monomer form is produced. However, the functional effect of abolishing glycosylation on this receptor is unknown. Several studies have indicated that loss of GPCR glycosylation can lead to improper folding and targeting, resulting in decreased function and compromised structure and stability (11). Loss of either N-terminal glycosylation site (Asn-2 or Asn-15) of rhodopsin is sufficient to cause loss of signal transduction despite no apparent change in localization or folding (21, 22). Additionally, mutating out the glycosylation site of a mouse OR (mOR-EG) was found to abolish its ability to localize to the membrane (10), indicating that this modification may be necessary for OR function. Because other heterologous expression systems (bacterial, insect, etc.) lack mammalian posttranslational machinery, purification of ORs from mammalian systems might be crucial for functional production.

In addition to the N-glycosylation site at Asn-5, hOR17-4 has a potential site at Asn-195. However, this residue does not appear to be glycosylated in this system as evidenced by: (*i*) the N5Q mutation causes a complete shift in mobility from the 32-kDa (glycosylated) form to the 30-kDa form, which corresponds to the mass of the deglycosylated hOR17-4 protein; (*ii*) MS analysis did not detect glycosylation at this site but did detect unglycosylated peptides containing Asn-195; and (*iii*) the consensus sequence is at the hypothetical EC2/TM5 border and thus is not likely to have the flexibility required for N-linked glycosylation. We did see a minor band running at ≈33 kDa for both the wild-type and N5Q mutant versions of hOR17-4 (Figs. 1*B* and 3*B*), which we have not yet ruled out as caused by potential Asn-195 glycosylation. Because this band does not appear to shift with N5Q mutation, were this band glycosylated it would be on Asn-195 alone (and not both sites). Should this be the case, a double mutant (N5Q, N195Q) might be advantageous, because it would eliminate both forms.

Detergent Screening. After a full-spectrum screening of >45 different detergents, we demonstrated the utility of the fos-choline-based detergents (most notably FC14) in extracting and solubilizing ORs. Fos-choline-12 was recently found to refold the integral membrane protein diacylglycerol kinase and maintain its functional state (23). Additionally, the *Escherichia coli* mechanosensitive ion channel MscS was successfully crystallized using FC14 and a high-resolution structure was obtained (24). We also previously reported using a wheat germ cell-free system to produce hOR17-4, mOR23, and mS51 and using FC14 to stabilize them for purifications and activity binding assays (25). The promise of this detergent class in future membrane protein research is underscored by our recent findings that identified the fos-choline series as the best detergent class for extracting and solubilizing the GPCR human chemokine receptors CCR3, CCR5, CXCR4, and CX3CR1 (26).

Future Perspectives. There have been a host of previous studies that have expressed and studied ORs in native and heterologous systems. Although purification of ORs has been attempted in bacterial (18) and Sf9 insect (27, 28) systems, they were unable to produce large quantities of native full-length OR. Our methods and results presented here constitute a cell-based platform for the production of milligram quantities of purified OR. Currently, we have demonstrated the production of >10 mg of full-length hOR17-4 in a stable tetracycline-inducible HEK293S cell line. The application of this method to other ORs may lead to a generalized procedure for obtaining large quantities of any OR in a rapid and simple manner. Such methods could prove extremely useful in discerning the elusive structure and functional mechanism of ORs, which would provide key insights into understanding the sense of smell at the molecular level. Additionally, the large-scale production of ORs is the prerequisite for their integration into OR-based biosensor devices.

Methods

Additional method details are provided in the *SI Text*.

BIOCHEMISTRY

Buffers and Solutions. Buffers used were as follows: phosphate-buffered saline (PBS), 137 mM NaCl, 2.7 mM KCl, 1.8 mM KH_2PO_4, 10 mM Na_2HPO_4 (pH 7.4); rinse buffer, PBS containing Complete Protease Inhibitor Mixture (Roche); solubilization buffer: rinse buffer containing 2% (wt/vol) FC14; wash buffer, PBS containing 0.2% FC14; elution buffer, wash buffer containing 100 μM Ac-TETSQVAPA-$CONH_2$ elution peptide. All detergents, including FC14, were purchased from Anatrace except digitonin, which was purchased from Sigma. All tissue culture and media components were purchased from Invitrogen unless otherwise noted. Sodium butyrate was purchased from Sigma.

Systematic Detergent Screening. For initial solubilization trials, the wild-type pcDNA4/To-hOR17-4-rho plasmid was transiently transfected into 15-cm tissue culture plates of HEK293S cells by using Lipofectamine 2000. After 48 h, cells were scrape-harvested and pooled. Cells were spun down and resuspended in ice-cold rinse buffer at a density of 2×10^7 cells per mL and then aliquotted into microcentrifuge tubes. Detergent was then added from stock solutions (10% wt/vol) such that the final concentration was 2%, except where noted. Care was taken not to vortex or pipette-mix the samples after detergent was added to avoid breaking cell nuclei. Samples were then rotated at 4 °C for 4 h before being centrifuged at 13,000 $\times$ *g* for 30 min to pellet insoluble material. Supernatants were then removed and subjected to dot blot and SDS/PAGE analysis with the rho1D4 mAb. Because dot blotting also detects aggregated/oligomerized receptor, the solubilization was quantified via SDS/PAGE Western blot analysis as the total amount of monomeric and dimeric hOR17-4 present, as determined by spot densitometry. Relative solubilization corresponds to the fold increase over DDM.

Immunoblotting and Total Protein Staining. Samples were assayed via SDS/PAGE under both reducing and denaturing conditions as described (5).

Immunoaffinity Purification. For immunoaffinity purification we used rho1D4 monoclonal antibody (Cell Essentials) chemically linked to CNBr-activated Sepharose 4B beads (GE Healthcare). The rho1D4 elution peptide Ac-TETSQVAPA-$CONH_2$ was synthesized by CBC Scientific. Rho1D4-Sepharose immunoaffinity purification has been described (5, 7, 25, 26).

Size Exclusion Chromatography. hOR17-4 proteins were subjected to gel filtration chromatography using a HiLoad 16/60 Superdex 200 column (GE Healthcare) on a Äkta Purifier FPLC system (GE Healthcare), as described (5). Pooled hOR17-4 elution fractions from the rho1D4 immunoaffinity purification were concentrated to 3 mg/mL by using a 10-kDa MWCO filter column (Millipore) and then applied to the Äkta system. After loading, the column was run with wash buffer at 0.3 mL/min and column flow-through was monitored via UV absorbance at 280, 254, and 215 nm. The molecular mass of hOR17-4-detergent complexes was estimated by calibrating the column with gel-filtration standard mixture (Bio-Rad). Molecular mass was correlated to retention volume by using a power law curve-fit.

CD Spectroscopy. Spectra were recorded at 15 °C with a CD spectrometer (Aviv Associates model 202). Far-UV CD spectra were measured over the wavelength range of 195 to 260 nm with a step size of 1 nm and an averaging time of 5 s. Near-UV CD spectra were measured over the wavelength range of 250 to 350 nm with a step size of 1 nm and an averaging time of 10 s. All spectra were the average of 5 replicate scans. Spectra shown for purified hOR17-4 were blanked to wash buffer (concentrated to same extent as hOR17-4 sample) to remove effects of the detergent FC14. Protein concentration was determined from the aromatic absorption in 6 M guanidinium HCl, pH 6.5 (29). All spectra were collected with a QS quartz sample cell (Hellma) with a path length of 1 mm. The secondary structural content was estimated by using the program K2D (www.embl-heidelberg.de/%7Eandrade/k2d.html).

SPR Odorant Binding Assay. All odorant binding experiments were performed at 25 °C on a Biacore A100 (GE Healthcare), which has a parallel flow configuration, allowing assay development (e.g., solubilization conditions) to be tested and optimized in parallel and multiplexed format. The sensor chip CM4, amine-coupling kit, HBS (10 mM Hepes, 0.15 M NaCl, pH 7.4) and PBS were from GE Healthcare. The detailed protocol (see *SI Text*) was adapted, with several key modifications, from that reported by Kaiser et al. (25).

ACKNOWLEDGMENTS. We thank members of the laboratory of H. Gobind Khorana, especially Philip J. Reeves and Prashen Chelikani, for their instruction regarding rho1D4 purification and providing the parental HEK293S cell line; Ioannis Papayannopoulos (Massachusetts Institute of Technology Koch Institute Proteomics Core Facility, Cambridge, MA) for assistance with mass spectrometry analysis; and Joyce and Roger Kiley of Flavor Sciences (Lenoir, NC) for providing pure odorants. S.Z. was supported by a John Simon Guggenheim Fellowship. B.L.C. was partly supported by the National Science Foundation– Massachusetts Institute of Technology Center for Bits and Atoms. This work was supported in part by a research grant from the ROHM Corporation, Kyoto, Japan.

1. Buck L, Axel R (1991) A novel multigene family may encode odorant receptors: A molecular basis for odor recognition. *Cell* 65:175–187.
2. Malnic B, Hirono J, Sato T, Buck LB (1999) Combinatorial receptor codes for odors. *Cell* 96:713–723.
3. Spehr M, et al. (2003) Identification of a testicular odorant receptor mediating human sperm chemotaxis. *Science* 299:2054–2058.
4. Hanson MA, Stevens RC (2009) Discovery of new GPCR biology: One receptor structure at a time. *Structure (London)* 17:8–14.
5. Cook BL, Ernberg KE, Chung H, Zhang S (2008) Study of a synthetic human olfactory receptor 17-4: Expression and purification from an inducible mammalian cell line. *PLoS ONE* 3:e2920.
6. Reeves PJ, Thurmond RL, Khorana HG (1996) Structure and function in rhodopsin: High-level expression of a synthetic bovine opsin gene and its mutants in stable mammalian cell lines. *Proc Natl Acad Sci USA* 93:11487–11492.
7. Reeves PJ, Kim JM, Khorana HG (2002) Structure and function in rhodopsin: A tetracycline-inducible system in stable mammalian cell lines for high-level expression of opsin mutants. *Proc Natl Acad Sci USA* 99:13413–13418.
8. Reeves PJ, Callewaert N, Contreras R, Khorana HG (2002) Structure and function in rhodopsin: High-level expression of rhodopsin with restricted and homogeneous N-glycosylation by a tetracycline-inducible *N*-acetylglucosaminyltransferase I-negative HEK293S stable mammalian cell line. *Proc Natl Acad Sci USA* 99:13419–13424.
9. Liu AH, Zhang X, Stolovitzky GA, Califano A, Firestein SJ (2003) Motif-based construction of a functional map for mammalian olfactory receptors. *Genomics* 81:443–456.
10. Katada S, Tanaka M, Touhara K (2004) Structural determinants for membrane trafficking and G protein selectivity of a mouse olfactory receptor. *J Neurochem* 90:1453–1463.
11. Wheatley M, Hawtin SR (1994) Glycosylation of G protein-coupled receptors for hormones central to normal reproductive functioning: Its occurrence and role. *Hum Reprod Update* 5:356–364.
12. Chelikani P, Reeves PJ, Rajbhandary UL, Khorana HG (2006) The synthesis and high-level expression of a β2-adrenergic receptor gene in a tetracycline-inducible stable mammalian cell line. *Protein Sci* 15:1433–1440.
13. Strop P, Brunger AT (2005) Refractive index-based determination of detergent concentration and its application to the study of membrane proteins. *Protein Sci* 14:2207–2211.
14. Chabre M, le Maire M (2005) Monomeric G protein-coupled receptor as a functional unit. *Biochemistry* 44:9395–9403.
15. Pilpel Y, Lancet D (1999) The variable and conserved interfaces of modeled olfactory receptor proteins. *Protein Sci* 8:969–977.
16. Andrade MA, Chacón P, Merelo JJ, Morán F (1993) Evaluation of secondary structure of proteins from UV circular dichroism using an unsupervised learning neural network. *Protein Eng* 6:383–390.
17. Liu X, Garriga P, Khorana HG (1996) Structure and function in rhodopsin: Correct folding and misfolding in two point mutants in the intradiscal domain of rhodopsin identified in retinitis pigmentosa. *Proc Natl Acad Sci USA* 93:4554–4559.
18. Kiefer H, et al. (1996) Expression of an olfactory receptor in *Escherichia coli*: Purification, reconstitution, and ligand binding. *Biochemistry* 35:16077–16084.
19. Jacquier V, Pick H, Vogel H (2006) Characterization of an extended receptive ligand repertoire of the human olfactory receptor OR17-40 comprising structurally related compounds. *J Neurochem* 97:537–544.
20. Fukuda MN, Papermaster DS, Hargrave PA (1979) Rhodopsin carbohydrate. Structure of small oligosaccharides attached at two sites near the NH_2 terminus. *J Biol Chem* 254:8201–8207.
21. Kaushal S, Ridge KD, Khorana HG (1994) Structure and function in rhodopsin: The role of asparagine-linked glycosylation. *Proc Natl Acad Sci USA* 91:4024–4028.
22. Zhu L, et al. (2004) A naturally occurring mutation of the opsin gene (T4R) in dogs affects glycosylation and stability of the G protein-coupled receptor. *J Biol Chem* 279:53828–53839.
23. Gorzelle BM, et al. (2002) Reconstitutive refolding of diacylglycerol kinase, an integral membrane protein. *Biochemistry* 38:16373–16382.
24. Bass RB, Strop P, Barclay M, Rees DC (2002) Crystal structure of *Escherichia coli* MscS, a voltage-modulated and mechanosensitive channel. *Science* 298:1582–1587.
25. Kaiser L, et al. (2008) Efficient cell-free production of olfactory receptors: Detergent optimization, structure, and odorant binding analyses. *Proc Natl Acad Sci USA* 105:15726–15731.
26. Ren H, et al. (2009) High-level production, solubilization, and purification of synthetic human GPCR chemokine receptors CCR5, CCR3, CXCR4, and CX3CR1. *PLoS ONE* 4:e4509.
27. Gat U, Nekrasova E, Lancet D, Natochin M (1994) Olfactory receptor proteins. Expression, characterization, and partial purification. *Eur J Biochem* 225:1157–1168.
28. Nekrasova E, Sosinskaya A, Natochin M, Lancet D, Gat U (1996) Overexpression, solubilization, and purification of rat and human olfactory receptors. *Eur J Biochem* 238:28–37.
29. Greenfield NJ (2006) Using circular dichroism spectra to estimate protein secondary structure. *Nat Protoc* 1:2876–2890.